Available online at www.sciencedirect.com
SCIENCE DIRECT®
PERGAMON
International Journal of Multiphase Flow 29 (2003) 1625–1642
International Journal of Multiphase Flow
www.elsevier.com/locate/ijmulflow

Permeabilities of unsaturated fractal porous media

Boming Yu [a,*], Jianhua Li [b], Zhihua Li [a], Mingqing Zou [a]

[a] *Department of Physics and The State Key Laboratory of Plastic Forming and Die & Mold Tech., Huazhong University of Science and Technology, Wuhan 430074, PR China*
[b] *Research Center of Biomedical Materials Engineering, Wuhan University of Technology, Wuhan 430070, China*

Received 15 January 2003; received in revised form 29 June 2003

Abstract

A fractal analysis of permeabilities for unsaturated fractal porous media is presented based on the fractal natures of pores in the media. Both the fractal *phase* permeabilities and the fractal *relative* permeabilities are derived and found to be a function of fractal dimension for tortuosity, pore area fractal dimension, fractal dimensions for wetting and non-wetting phases, saturation and microstructural parameters. The proposed fractal models for permeabilities, both the phase permeabilities and the relative permeabilities, do not contain any empirical constant. To verify the validity of the present analysis, the predicted relative permeability data are compared with those of the existing measurements, and excellent agreement between the model predictions and existing experimental data is found.

Keywords: Fractal; Permeability; Porous media; Multiphase flow

1. Introduction

The permeabilities for porous media, both saturated and unsaturated, have received much attention (De Wiest, 1969; Bear, 1972; Bowles, 1984; Jumikis, 1984; Kaviany, 1995; Panfilov, 2000) due to practical applications including chemical engineering, soil science and engineering, oil production, polymer composite molding and heat pipes etc. Since the microstructures of real porous media are usually disordered and extremely complicated, this makes it very difficult to analytically find the permeability of the media especially for unsaturated (or multiphase) porous media.

* Corresponding author. Tel.: +86-27-875-421-53; fax: +86-27-875-454-38.
E-mail address: yu3838@public.wh.hb.cn (B. Yu).

0301-9322/$ - see front matter
doi:10.1016/S0301-9322(03)00140-X

Conventionally, the permeabilities of porous media were found by experiments (Levec and Saez, 1986; Sasaki et al., 1987; Wang et al., 1994; Wu et al., 1994; Shih and Lee, 1998; Chen et al., 2000). Besides, much effort was devoted to numerical simulations (Benzi et al., 1992; Martys and Chen, 1996; Chen and Doolen, 1998; Adler and Thovert, 1998; Adler and Berkowitz, 2000; Pandey et al., 2001; Ngo and Tamma, 2001). However, the results from either experiments or numerical simulations are usually expressed as correlations with one or more empirical constants or as curves, and the mechanisms behind the phenomena are thus often ignored. In order to get a better understanding of the mechanisms for permeability, an analytical solution for permeability of porous media becomes a challenging task.

Yu and Lee (2000) developed a simplified analytical model for evaluating the permeabilities of porous fabrics used in liquid composite molding. This permeability model, which is related to porosity and architectural structures of porous fabrics, is based on the one-dimensional Stokes flow in macropores between fiber tows and on the one-dimensional Brinkman flow in micropores inside fiber tows. Good agreement between theoretical predictions and experimental results was found. However, this model may only apply to those media whose macropores can be simplified as one-dimensional channels. So this and several other models may not be applicable to random/disordered porous media. In addition, this model is only suitable to saturated porous media.

Katz and Thompson (1985) are the first to present the experimental evidence indicating that the pore spaces of a set of sandstone samples are fractals and are self-similar over 3–4 orders of magnitude in length extending from 10 Å to 100 μm. They argued that the pore volume is a fractal with the same fractal dimension as the pore–rock interface. This conclusion was supported by correctly predicting the porosity from the fractal dimension, which was measured by a log–log plot of number of pores versus the pore size. Krohn and Thompson (1986) also showed a set of sandstone pores and found that they are fractals and follow the fractal power laws.

Adler (1985) numerically simulated the transport problem by applying a percolation model in a fractal object, but no relation between the simulated results and fractal dimension was reported. After 10 years, Adler (1996) concluded that the permeability in real porous media can be expressed as $K = K(\phi, D_f, \ldots)$. However, no quantitative expression was given. Pitchumani and Ramakrishnan (1999) proposed a fractal model for permeability of real porous fiber preforms. This may be the first analytical model for permeability of fractal porous media and there is no empirical constant in their model. Unfortunately, this model is found to be completely in error (Yu, 2001).

Recently, Yu and Cheng (2002) developed a fractal permeability model for bi-dispersed (saturated) porous media based on the fractal characteristics of pore sizes of the media, and this fractal model is also applicable to porous anisotropic fabrics (Yu et al., 2002, 2003). Although this model does not contain any empirical constant and good agreement is found between the model predictions and experimental data, it is not applicable to unsaturated porous media. The saturated porous medium is, in fact, only the special case of the unsaturated porous medium. It is, therefore, more meaningful to develop an analytical solution for permeability of unsaturated (or multiphase) porous media.

It should be noted that not all porous media are fractals, only those porous media whose pore structures and pore size distributions are random and disordered may be fractals. In this paper, we focus our attention on the derivation of a fractal analytical model for permeabilities of unsaturated fractal porous media based on the fact that the porous media in nature are fractals

(Katz and Thompson, 1985; Krohn and Thompson, 1986; Young and Crawford, 1991; Perfect and Kay, 1991; Smidt and Monro, 1998; Yu and Li, 2001; Yu et al., 2001; Yu and Cheng, 2002; Yu et al., 2002). In the next section we give the detailed description of the fractal characteristics of microstructures of fractal porous media, which are the theoretical bases for the present fractal analysis of permeabilities.

2. The description of microstructures of fractal porous media

Euclidean geometry describes ordered objects such as points, curves, surfaces and cubes using integer dimensions 0, 1, 2 and 3, respectively. Their measures are invariant with respect to the unit of measurement used. However, numerous objects found in nature (Mandelbrot, 1982) such as rough surfaces, coastlines, mountains, rivers, lakes and islands, are disordered and irregular, and they do not follow the Euclidean description due to the scale-dependent measures of length, area and volume. These objects are called fractals, and the dimensions of such objects are non-integral and called *Hausdorff dimension*, or simply *fractal dimension*. The geometry structures such as Sierpinski gasket, Sierpinski carpet and Koch curve are the examples of the exactly self-similar fractals or regular fractals, which exhibit the self-similarity over an infinite range of length scales. Their dimensions are also called *similarity* dimensions (Feder, 1988). However, exactly self-similar fractals in a global sense are rarely found in nature. Many objects found in nature are not exactly self-similar, such as coastlines, islands on earth, they are statistically self-similar and they are called the statistical fractals. These objects exhibit the self-similarity in some average sense and over a certain local range of length scales, L. The fractal dimensions used in this paper are applicable to both the exactly self-similar fractals (such as Sierpinski gasket, Sierpinski carpet and Koch curve) and the statistical fractals (such as fractal/random porous media).

Porous media such as soil, sandstones in oil reservoir, packed beds in chemical engineering, fabrics used in liquid composite molding and wicks in heat pipes consist of numerous irregular pores of different sizes spanning several orders of magnitude in length scales. The pore microstructures, both the pore sizes and the pore-interfaces, of such porous media exhibit the fractal characteristics (Katz and Thompson, 1985; Krohn and Thompson, 1986; Young and Crawford, 1991; Perfect and Kay, 1991; Smidt and Monro, 1998; Yu and Li, 2001; Yu et al., 2001; Yu and Cheng, 2002; Yu et al., 2002), and these media are called fractal porous media. The present work only deals with these media. For simplicity, we here use the word "porous media" to represent the word "fractal porous media".

In should be noted that in some cases, as pointed by Feder (1988), some fractal objects such as Brownian motion exhibits the fractal character with different scaling ratios in different directions, this character is called "self-affinity". However, our previous study (Yu et al., 2001) showed that for porous fabrics, although their microstructures and permeabilities are anisotropic, their fractal dimensions are approximately the same in different directions, this means that the "self-affinity" for porous media can be neglected, as many studies by Katz and Thompson (1985), Krohn and Thompson (1986), Young and Crawford (1991), Perfect and Kay (1991), Smidt and Monro (1998), Yu and Li (2001), Yu et al. (2001), Yu and Cheng (2002) and Yu et al. (2002). Therefore, we neglect the "self-affinity" in this work.

The pore in porous media plays a remarkable role in fluid flow and heat transfer in porous media. The conventional method for description of characteristics of porous media is based on the volume average (Kaviany, 1995) over the considered medium, and the significant influence of microstructures on flow is thus ignored. Fortunately, the fractal natures of pores and pore fluids may provide us with a better understanding of the mechanisms of flow and transport properties, such as the permeability in porous media.

It is known that the cumulative size-distribution of islands on the earth's surface follows the power law $N(A > a) \sim a^{-D/2}$ (Mandelbrot, 1982), where N is the total number of islands of area (A) greater than a, and D is the fractal dimension of the surface. The equality in the above cumulative size-distribution of islands on the earth's surface can be invoked by using $a_{\max}$ to be the largest island to yield (Majumdar and Bhushan, 1990)

$$N(A \geqslant a) = \left(\frac{a_{\max}}{a}\right)^{D_f/2} \tag{1}$$

Eq. (1) implies that there is only one largest island on the earth's surface, this is consistent with the physical situation. Marjumdar and Bhushan used this power law Eq. (1) to describe the contact spots on engineering surfaces, where $a_{\max} = g\lambda_{\max}^2$, $a = g\lambda^2$, with λ being the diameter of a spot and g being a geometry factor. Compared with the islands on the earth's surface or spots on engineering surfaces, the pores in porous media are analogous to the islands on the earth's surface and to the spots on engineering surfaces. The cumulative size-distribution of pores whose sizes are greater than or equal to λ has also been proven to follow the fractal scaling law (Yu and Cheng, 2002; Yu et al., 2002).

$$N(L \geqslant \lambda) = \left(\frac{\lambda_{\max}}{\lambda}\right)^{D_f} \tag{2}$$

where D_f is the pore area fractal dimension, $1 < D_f < 2$ and $\lambda_{\max}$ is the maximum pore size. Differentiating Eq. (2) with respect to λ results in the number of pores whose sizes are within the infinitesimal range λ to $\lambda + d\lambda$,

$$-dN = D_f \lambda_{\max}^{D_f} \lambda^{-(D_f+1)} d\lambda \tag{3}$$

The negative sign in Eq. (3) implies that the island or pore number decreases with the increase of island or pore size, and $-dN > 0$. Eq. (2) describes the scaling relationship of the cumulative pore population. The total number of pores or islands or spots, from the smallest diameter $\lambda_{\min}$ to the largest diameter $\lambda_{\max}$, can be obtained from Eq. (2) as (Yu and Li, 2001; Yu and Cheng, 2002; Yu et al., 2002)

$$N_t(L \geqslant \lambda_{\min}) = \left(\frac{\lambda_{\max}}{\lambda_{\min}}\right)^{D_f} \tag{4}$$

Dividing Eq. (2) by Eq. (4) gives

$$-\frac{dN}{N_t} = D_f \lambda_{\min}^{D_f} \lambda^{-(D_f+1)} d\lambda = f(\lambda)\, d\lambda \tag{5}$$

where $f(\lambda) = D_f \lambda_{\min}^{D_f} \lambda^{-(D_f+1)} \geqslant 0$ is the probability density function. Patterned after probability theory, the probability density function, $f(\lambda)$, should satisfy the following relationship:

$$\int_0^{\infty} f(\lambda)\,\mathrm{d}\lambda = \int_{\lambda_{\min}}^{\lambda_{\max}} f(\lambda)\,\mathrm{d}\lambda = 1 - \left(\frac{\lambda_{\min}}{\lambda_{\max}}\right)^{D_f} \equiv 1 \tag{6}$$

It is clear that Eq. (6) holds if and only if (Yu and Li, 2001)

$$\left(\frac{\lambda_{\min}}{\lambda_{\max}}\right)^{D_f} \cong 0 \tag{7}$$

is satisfied. Eq. (7) implies that $\lambda_{\min} << \lambda_{\max}$ must be satisfied for fractal analysis of a porous medium, otherwise the porous medium is a non-fractal medium. For example, if $\lambda_{\min} = \lambda_{\max}$, both Eqs. (6) and (7) do not hold. Eq. (7) can be considered as a criterion (Yu and Li, 2001) whether a porous medium can be characterized by fractal theory and technique. This means that if Eq. (7) does not hold, the porous medium is a non-fractal medium, and the fractal theory and technique are not applicable to the medium. Fortunately, in general, $\lambda_{\min}/\lambda_{\max} \sim 10^{-2}$ or $<10^{-2}$ in porous media, thus Eq. (7) holds for porous media. Thus, the fractal theory and technique can be used to analyze the characters of porous media.

If we take the Sierpinski carpet or Sierpinski gasket as a porous medium model, it is easy to see that the following relation holds:

$$D_f = 2 - \frac{\ln \varepsilon}{\ln \frac{\lambda_{\min}}{\lambda_{\max}}} \tag{8a}$$

where D_f $(1 < D_f < 2)$ is the fractal dimension ε is the porosity, $\lambda_{\min}$ and $\lambda_{\max}$ are the lower and upper limits of self-similar regions. For Sierpinski carpet $D_f = 1.8928$ and for Sierpinski gasket $D_f = 1.5850$. For example, in two dimensions for the 0-stage Sierpinski carpet, $\lambda_{\min}/\lambda_{\max} = 1/3$ and $\varepsilon = 8/9$, the fractal dimension can be found to be $D_f = 1.8928$ from Eq. (8a); for the 1-stage Sierpinski carpet, $\varepsilon = (8/9)^2$, $\lambda_{\min}/\lambda_{\max} = 1/9$, and the fractal dimension can be also found to be $D_f = 1.8928$ from Eq. (8a). This is expected. For any stage Sierpinski carpet and Sierpinski gasket, Eq. (8a) holds. For the three-dimensional Sierpinski carpets and Sierpinski gaskets, Eq. (8a) can be extended to yield

$$D_f = 3 - \frac{\ln \varepsilon}{\ln \frac{\lambda_{\min}}{\lambda_{\max}}} \tag{8b}$$

where $2 < D_f < 3$. Combining Eqs. (8a) and (8b), a unified relation between the fractal dimension and porosity can be obtained as (Yu and Li, 2001)

$$D_f = d - \frac{\ln \varepsilon}{\ln \frac{\lambda_{\min}}{\lambda_{\max}}} \tag{9}$$

where d is the Euclidean dimension, and $d = 2$ and 3 in the two- and three-dimensional spaces, respectively. Eq. (9) exactly holds for exact self-similar fractal geometries, such as Sierpinski carpet and Sierpinski gasket ($\lambda_{\max}$ and $\lambda_{\min}$ are the upper and lower limits of self-similarity, respectively). But Eq. (9) approximately holds for random or disordered fractal porous media (for porous media, $\lambda_{\max}$ and $\lambda_{\min}$ are the maximum and minimum pore diameters, respectively, in a unit cell or in a sample, this implies that the statistical self-similarity exists in the range of $\lambda_{\min} \sim \lambda_{\max}$ in porous media), and the detailed derivations are given elsewhere (Yu and Li, 2001).

Eq. (9) shows that the pore area fractal dimension is a function of porosity and microstructures, λ_{min} and λ_{max}.

Onoda and Toner (1986) presented a model for fractal dimension of fractal objects, this model is expressed as:

$$D = d + \frac{\ln p}{\ln S} \tag{C}$$

where p is the packing fraction of the previous generation of agglomerates in an agglomerate, i.e. relative volume fraction of any generation of agglomerates, and is the same from generation to generation. It is not the packing fraction of particles in the *overall* structure. S in Eq. (C) is a factor by which each successive generation of agglomerates is always larger than the previous. It is seen that the porosity ϕ (corresponding to the packing fraction of particles in the overall structure) in Eq. (9) has the different meaning from p in Eq. (C). In addition, λ_{min} and λ_{max} in Eq. (9) are the lower limit and upper limits of self-similar regions, which are also different from S in Eq. (C). Both Eqs. (C) and (9) can be easily applied to calculate the fractal dimensions of exact fractal geometries, such as Sierpinski carpet and Sierpinski gasket. However, when a statistically self-similar fractal medium, such as a random fractal porous medium, is concerned, p and S in Eq. (C) usually cannot be easily determined. While the porosity ϕ or packing fraction of particles in the *overall* structure can be easily found/measured, and λ_{min} and λ_{max} in a sample or a unit cell can be also easily measured by instrument or by box-counting method. Then, Eq. (9) can be applied to determine the fractal dimension of the structure.

Most recently, Yu and Li (in press) derived the analytical expressions for the phase fractal dimensions of unsaturated porous media, the expressions are given as

$$D_{f,w} = d + \frac{\ln(S_w \varepsilon)}{\ln \frac{\lambda_{max}}{\lambda_{min}}} \tag{10a}$$

$$D_{f,g} = d + \frac{\ln[(1 - S_w)\varepsilon]}{\ln \frac{\lambda_{max}}{\lambda_{min}}} \tag{10b}$$

where S is the saturation, the subscripts w and g represent the wetting (e.g. water) and non-wetting (e.g. gas) phases, respectively. Eq. (10a) indicates that when $S_w = 1$, Eq. (10a) will be reduced to Eq. (9), meaning that the medium becomes a single phase/saturated porous one. If $S_w = 0$, Eq. (10b) will be also reduced to Eq. (9) and the medium is also a single phase/saturated porous one. It can be seen that Eq. (9) is only a special case of saturation $S_w = 1$ in Eq. (10a) or $S_w = 0$ in Eq. (10b), and Eq. (10) is the general expression for fractal dimensions of porous media, both saturated and unsaturated porous media.

A porous medium having various pore sizes can be considered as a bundle of tortuous capillary tubes with variable cross sectional areas. Let the diameter of a capillary in the medium be λ and its tortuous length along the flow direction be $L_t(\lambda)$. Due to the tortuous nature of the capillary, $L_t(\lambda) \geqslant L_0$, with L_0 being the representative length. For a straight capillary, $L_t(\lambda) = L_0$. Wheatcraft and Tyler (1988) developed a fractal scaling/tortuosity relationship for flow through heterogeneous media, and the scaling relationship is given by $L_t(\delta) = \delta^{1-D_T} L_0^{D_T}$, where δ is the length scale of measurement. We argue that the diameters of capillaries are analogous to the length scales δ, which means that the smaller the diameter of a capillary, the longer the capillary. Therefore, the

relationship between the diameter and length of capillaries also exhibits the similar fractal scaling law:

$$L_t(\lambda) = \lambda^{1-D_T} L_0^{D_T} \tag{11}$$

where D_T is the fractal dimension for tortuosity, with $1 < D_T < 2$, representing the extent of convolutedness of capillary pathways for fluid flow through a medium. Note that $D_T = 1$ represents a straight capillary path, and a higher value of D_T corresponds to a highly tortuous capillary. In the limiting case of $D_T = 2$, we have a highly tortuous line that fills a plane (Wheatcraft and Tyler, 1988). Eq. (11) diverges as $\lambda \to 0$, which is one of the properties of fractal streamlines.

The fractal dimensions D_f and D_T, defined by Eqs. (2) and (11) respectively, are called *Hausdorff dimension* (often called *fractal dimension*) according to the definition given by Mandelbrot (1982). Since Eqs. (8)–(10) are also based on Eq. (2), the fractal dimensions, D_f, $D_{f,w}$ and $D_{f,g}$, in Eqs. (8)–(10) are also called *Hausdorff dimension* (or simply *fractal dimension*). On the other hand, since these fractal dimensions can be determined by the box-counting method, they are also named *box-counting dimension* or *box dimension* (Feder, 1988).

Eqs. (2)–(4) and (7)–(11), which present a complete description of the fractal characters of unsaturated porous media, form the basis of the present fractal analysis of permeabilities, which will be derived in the following section.

3. Fractal permeabilities for unsaturated porous media

Consider a unit cell consisting of a bundle of tortuous capillary tubes with variable cross sectional area, and each capillary tube is partially filled with the wetting and non-wetting phase fluids. This is the typical state for unsaturated porous media. According to the literature by Kaviany (1995), at very low saturations the wetting phase becomes disconnected (or immobile), and at very high saturations the non-wetting phase becomes disconnected. So, in this work we assume that the saturations are not very low and fluids in each capillary keep continuous. Since pore size distributions in porous media have been proven to be fractals and their fractal characters can be described by Eqs. (2)–(4) and (7)–(11), we assume that the wetting and non-wetting phases in porous media are all fractals and they also follow Eqs. (2)–(4) and (7)–(11). We also have the following assumptions similar to those given by Kaviany (1995) for the present analysis:

(1) The Darcy (Stokes) flow is applicable with a negligible interfacial drag in two-phase porous media.
(2) The body force is neglected.
(3) The liquid flow is not coupled with gas flow.
(4) The viscosities of liquid phase and gas phase are independent of each other.

We also assume that the wetting phase and the non-wetting phase flows through tortuous paths with approximately the same tortuosity as the single-phase flow, i.e. $D_T = D_{T,w} = D_{T,g} = 1.10$ (Yu and Cheng, 2002) measured from the box-counting method. Wheatcraft and Tyler (1988) performed the Monte Carlo simulations on an ensemble average fractal travel distance $L_t(\delta)$ versus

scale of δ for the fractal random walk model to simulate the dispersivity in heterogeneous media. They obtained the tortuosity fractal dimension of $D_T = 1.081$, which is very close to the value of $D_T = 1.10$ taken in this work.

The flow rate through a single tortuous capillary is given by modifying the well known Hagen–Poiseulle equation (Denn, 1980) to give

$$q(\lambda) = G\frac{\Delta P}{L_t(\lambda)}\frac{\lambda^4}{\mu} \tag{12}$$

where $G = \pi/128$ is the geometry factor for flow through a circular capillary, λ is the hydraulic diameter of a single capillary tube, μ is the viscosity of the fluid, ΔP is the pressure gradient, and L_t is the length of the tortuous capillary tube. Thus, the flow rate for each phase in a single tortuous capillary can be written as

$$q_w(\lambda_w) = G\frac{\Delta P_w}{L_t(\lambda_w)}\frac{\lambda_w^4}{\mu_w} \tag{13a}$$

$$q_g(\lambda_g) = G\frac{\Delta P_g}{L_t(\lambda_g)}\frac{\lambda_g^4}{\mu_g} \tag{13b}$$

The total volumetric flow rates for each phase, Q_w and Q_g, through the unit cell are the sums of the flow rates through all the individual capillaries, respectively. The total flow rate for each phase can be obtained by integrating the individual flow rates, $q_w(\lambda_w)$ and $q_g(\lambda_g)$, over the entire range of pore channel sizes from the minimum pore channel $\lambda_{min,w}$ (and $\lambda_{min,g}$) to the maximum pore channel $\lambda_{max,w}$ (and $\lambda_{max,g}$) in a unit cell. According to Eqs. (3), (11) and (13a), we have

$$\begin{aligned} Q_w &= -\int_{\lambda_{min,w}}^{\lambda_{max,w}} q(\lambda_w)\,dN(\lambda_w) \\ &= G\frac{\Delta P_w}{\mu_w}\frac{A}{L_0}\frac{L_0^{1-D_T}}{A}\frac{D_{f,w}}{3+D_T-D_{f,w}}\lambda_{max,w}^{3+D_T}\left[1-\left(\frac{\lambda_{min,w}}{\lambda_{max,w}}\right)^{D_{f,w}}\left(\frac{\lambda_{min,w}}{\lambda_{max,w}}\right)^{3+D_T-2D_{f,w}}\right] \end{aligned} \tag{14}$$

where $D_{f,w}$ is the area fractal dimension for the wetting phase given by Eq. (10a) and $1 < D_{f,w} < 2$ in two dimensions. Since $1 < D_T < 2$ and $1 < D_{f,w} < 2$, the exponent $3 + D_T - 2D_{f,w} > 0$ and $0 < (\frac{\lambda_{min,w}}{\lambda_{max,w}})^{3+D_T-2D_{f,w}} < 1$. Also, according to the Yu and Li's criterion Eq. (7) (Yu and Li, 2001), $(\frac{\lambda_{min}}{\lambda_{max}})^{D_f} \cong 0$, we also have $(\frac{\lambda_{min,w}}{\lambda_{max,w}})^{D_{f,w}} \cong 0$ (because usually $\frac{\lambda_{min}}{\lambda_{max}} \sim 10^{-2}$, thus $\frac{\lambda_{min,w}}{\lambda_{max,w}} \sim 10^{-2}$). It follows that Eq. (14) can be reduced to

$$Q_w = G\frac{\Delta P_w}{\mu_w}\frac{A}{L_0}\frac{L_0^{1-D_T}}{A}\frac{D_{f,w}}{3+D_T-D_{f,w}}\lambda_{max,w}^{3+D_T} \tag{15}$$

Using Darcy's law, we obtain the permeability expression for the wetting phase in an unsaturated porous medium as follows:

$$K_w = \frac{\mu_w L_0 Q_w}{\Delta P_w A} = G\frac{L_0^{1-D_T}}{A}\frac{D_{f,w}}{3+D_T-D_{f,w}}\lambda_{max,w}^{3+D_T} \tag{16}$$

which indicates that the wetting phase permeability is a function of the fractal dimensions $D_{f,w}$, D_T and structural parameters, A, L_0 and $\lambda_{max,w}$.

It can be found that although both the integration of Eq. (14) and the phase permeability model Eq. (16) are very simple, the mechanisms affecting the flow rate and permeability are quantitatively related. However, the conventional numerical methods such as lattice gas (Pandey et al., 2001), lattice Boltzmann method (Chen and Doolen, 1998) and Effective Medium analysis (Adler and Berkowitz, 2000) need artificially construct a porous medium or random lattice/medium, then Monte Carlo simulations or iterations are performed to solve more sophisticated equations/models (usually, a set of equations, e.g. N-S equations) for effective conductivity (such as permeability). While the present model is based on a real fractal porous medium, *not* based on an artificial porous medium, to solve a simple model given by Eqs. (14) and (16) for permeability. The second significantly different feature between the conventional numerical methods such as Effective Medium analysis (Adler and Berkowitz, 2000) and the present fractal analysis is that the Effective Medium analysis assumes the lattice bond conductivities distributed lognormally while the present fractal analysis is based on the pore size distribution following the fractal power laws (Katz and Thompson, 1985; Krohn and Thompson, 1986; Young and Crawford, 1991; Perfect and Kay, 1991; Smidt and Monro, 1998; Yu and Li, 2001; Yu et al., 2001; Yu et al., 2002; Yu and Cheng, 2002). The third significant difference between the conventional numerical methods such as Effective Medium analysis (Adler and Berkowitz, 2000), lattice gas (Pandey et al., 2001) and the present fractal analysis is that a comparison with experimental permeability data was not given in their methods, while our present fractal analysis presents such a comparison (see Section 4). Therefore, the validity of their analysis and lognormal distribution assumption for bond conductivities should be further verified by a comparison with experimental data.

Similarly, the permeability expression for the non-wetting phase in an unsaturated porous medium can be obtained as

$$K_g = \frac{\mu_g L_0 Q_g}{\Delta P_g A} = G \frac{L_0^{1-D_T}}{A} \frac{D_{f,g}}{3 + D_T - D_{f,g}} \lambda_{max,g}^{3+D_T} \tag{17}$$

where $D_{f,g}$ is the area fractal dimension for the non-wetting phase given by Eq. (10b) and $1 < D_{f,g} < 2$ in two dimensions.

For straight capillaries, $D_T = 1$, Eqs. (16) and (17) can be reduced to

$$K_w = G \frac{1}{A} \frac{D_{f,w}}{4 - D_{f,w}} \lambda_{max,w}^4 \tag{18}$$

and

$$K_g = G \frac{1}{A} \frac{D_{f,g}}{4 - D_{f,g}} \lambda_{max,g}^4 \tag{19}$$

respectively. Eqs. (15)–(19) present the phase flow rate (Q_w) and *phase* permeabilities (K_w and K_g) in an unsaturated porous medium. Eqs. (15)–(19) indicate that the phase flow rate and phase permeabilities are very sensitive to the maximum phase channel sizes $\lambda_{max,w}$ and $\lambda_{max,g}$. It is also shown that the higher the fractal dimensions $D_{f,w}$ and $D_{f,g}$, the larger the flow rate and the phase permeability values. From Eqs. (15)–(19), it can be seen that the flow rate and the phase

permeabilities will reach the maximum possible values as the fractal dimensions $D_{f,w}$ and $D_{f,g}$ approach their maximum possible value of 2. This is in consistence with fractal theory.

For saturated porous media, each capillary is filled with a single fluid and thus we have $S_w = 1$ in Eq. (10a) or $S_w = 0$ in Eq. (10b), Eq. (10) will be reduced to Eq. (9) and $\lambda_{max,w} = \lambda_{max,g} = \lambda_{max}$, $\lambda_{min,w} = \lambda_{min,g} = \lambda_{min}$. Then we have the permeabilities for saturated porous media

$$K = G\frac{L_0^{1-D_T}}{A}\frac{D_f}{3+D_T-D_f}\lambda_{max}^{3+D_T} \tag{20}$$

For straight capillaries, $D_T = 1$, Eq. (20) can be reduced to

$$K = G\frac{1}{A}\frac{D_f}{4-D_f}\lambda_{max}^{4} \tag{21}$$

Eqs. (20) and (21) describe the permeabilities for saturated porous media. It is seen that Eqs. (16)–(19) are the general expressions for permeabilities of unsaturated porous media, and Eqs. (20) and (21) are the special cases of unsaturated porous media. Eqs. (20) and (21) are also called the *absolute* permeabilities.

The permeations of both wetting and non-wetting fluids play important roles in unsaturated (or multiphase) porous media. Muskat and Meres (1936) recommended that the phase permeabilities K_w and K_g be treated as isotropic and given by

$$K_w = Kk_{rw} \tag{22}$$

$$K_g = Kk_{rg} \tag{23}$$

or

$$k_{rw} = K_w/K \tag{24}$$

$$k_{rg} = K_g/K \tag{25}$$

where k_{rw} and k_{rg} are the *relative* permeabilities of the wetting and non-wetting phases, respectively.

The permeations for unsaturated porous media are usually expressed as the *relative* permeabilities. Combining Eqs. (16), (17), (20), (24) and (25) yields

$$k_{rw} = \frac{K_w}{K} = \frac{3+D_T-D_f}{3+D_T-D_{f,w}}\frac{D_{f,w}}{D_f}\left(\frac{\lambda_{max,w}}{\lambda_{max}}\right)^{3+D_T} \tag{26}$$

$$k_{rg} = \frac{K_g}{K} = \frac{3+D_T-D_f}{3+D_T-D_{f,g}}\frac{D_{f,g}}{D_f}\left(\frac{\lambda_{max,g}}{\lambda_{max}}\right)^{3+D_T} \tag{27}$$

It is evident that the relative permeability is a function of fractal dimensions D_f, D_T and $D_{f,w}$ (or $D_{f,g}$), and microstructural parameters, λ_{max}, $\lambda_{max,w}$ (or $\lambda_{max,g}$). There is no any empirical constant in this fractal relative permeability model. The fractal dimensions D_f, $D_{f,w}$, $D_{f,g}$ and D_T are given by Eqs. (9)–(11). Once the ratios of $\lambda_{max,w}/\lambda_{max}$ and $\lambda_{max,g}/\lambda_{max}$ are found, the relative permeabilities can be determined. In the following, we will give the detailed derivation for the ratios of $\lambda_{max,w}/\lambda_{max}$ and $\lambda_{max,g}/\lambda_{max}$.

Fig. 1 shows a schematic of the cross section of a capillary tube partially filled with water and gas. From Fig. 1, we can obtain the pore volume V_p and the volume, V_w, occupied by water or wetting phase as

$$V_p = \pi\lambda^2/4 \tag{28}$$

and

$$V_w = V_p - V_g = \pi\lambda^2/4 - \pi\lambda_g^2/4 \tag{29}$$

respectively, where λ and λ_g are the diameter of a capillary pathway and the diameter of non-wetting (e.g. gas) phase pathway, and V_g is the volume occupied by non-wetting fluid. According to the definition (Bear, 1972) for saturation S_w, we have

$$S_w = \frac{V_w}{V_p} = 1 - \left(\frac{\lambda_g}{\lambda}\right)^2 \tag{30}$$

and

$$S_g = \frac{V_g}{V_p} = \left(\frac{\lambda_g}{\lambda}\right)^2 \tag{31}$$

Obviously, Eqs. (30) and (31) satisfies $S_w + S_g = 1$ and this is expected. From Eqs. (30) and (31) the diameter for non-wetting fluid (such as gas) can be expressed as

$$\lambda_g = \lambda\sqrt{S_g} = \lambda\sqrt{1 - S_w} \tag{32}$$

Eq. (32) denotes that $\lambda_g = 0$ as $S_w = 1$ and $\lambda_g = \lambda$ as $S_w = 0$, and vice versa. This is expected and is consistent with physical situation.

The volume, V_w, occupied by the wetting fluid (such as water) can be written as

$$V_w = \pi\lambda^2/4 - \pi\lambda_g^2/4 = \pi\lambda_w^2/4 \tag{33}$$

where λ_w is the *effective* diameter of wetting fluid occupying the cross section of a capillary pathway. Again, according to the definition of saturation

$$S_w = V_w/V_p = \lambda_w^2/\lambda^2 \tag{34}$$

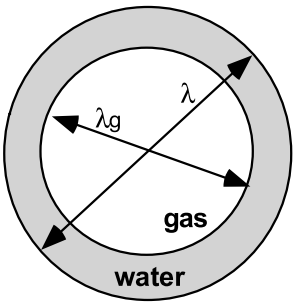

Fig. 1. A schematic of the cross section of a capillary tube partially filled with water and gas.

This results in

$$\lambda_w = \lambda\sqrt{S_w} \tag{35}$$

Eq. (35) indicates that $\lambda_w = 0$ as $S_w = 0$ and $\lambda_w = \lambda$ as $S_w = 1$, and vice versa. This is again expected and is consistent with physical situation. Usually, $0 < S_w < 1$ such as the saturation in soil, in which pores are partially filled with fluid such as water, i.e. the two phases (e.g. water and gas) coexist in soil. From Eqs. (32) and (35), we can directly write the effective maximum and the smallest diameters for wetting and non-wetting fluids in maximum and smallest pores (or capillary tubes) as

$$\lambda_{max,w} = \lambda_{max}\sqrt{S_w} \quad \text{or} \quad \lambda_{max,w}/\lambda_{max} = \sqrt{S_w} \tag{36a}$$

$$\lambda_{min,w} = \lambda_{min}\sqrt{S_w} \quad \text{or} \quad \lambda_{min,w}/\lambda_{min} = \sqrt{S_w} \tag{36b}$$

$$\lambda_{max,g} = \lambda_{max}\sqrt{1 - S_w} \quad \text{or} \quad \lambda_{max,g}/\lambda_{max} = \sqrt{1 - S_w} \tag{36c}$$

$$\lambda_{min,g} = \lambda_{min}\sqrt{1 - S_w} \quad \text{or} \quad \lambda_{min,g}/\lambda_{min} = \sqrt{1 - S_w} \tag{36d}$$

It is seen that if we insert Eqs. (36a)–(36d) into Eq. (9), and apply the relations: $S_w = V_w/V_p = (V_w/V_t)/(V_p/V_t) = \varepsilon_w/\varepsilon$ or $\varepsilon_w = S_w\varepsilon$, and $\varepsilon_g = S_g\varepsilon = (1 - S_w)\varepsilon$, we can also obtain Eq. (10), i.e.

$$D_{f,w} = d - \frac{\ln \varepsilon_w}{\ln \frac{\lambda_{min,w}}{\lambda_{max,w}}} = d - \frac{\ln(S_w\varepsilon)}{\ln \frac{\lambda_{min}\sqrt{S_w}}{\lambda_{max}\sqrt{S_w}}} = d + \frac{\ln(S_w\varepsilon)}{\ln \frac{\lambda_{max}}{\lambda_{min}}} \tag{10a}$$

This is exactly Eq. (10a). Similarly, we can obtain Eq. (10b).

We can now turn our attention again on the relative permeabilities for wetting and non-wetting phases. Inserting Eqs. (36a) and (36c) into Eqs. (26) and (27), respectively, we arrive at

$$k_{rw} = \frac{K_w}{K} = \frac{3 + D_T - D_f}{3 + D_T - D_{f,w}} \frac{D_{f,w}}{D_f} S_w^{(3+D_T)/2} \tag{37}$$

$$k_{rg} = \frac{K_g}{K} = \frac{3 + D_T - D_f}{3 + D_T - D_{f,g}} \frac{D_{f,g}}{D_f} (1 - S_w)^{(3+D_T)/2} \tag{38}$$

It is evident that the relative permeability k_{rw} (or k_{rg}) is a function of saturation S_w and fractal dimensions D_f, D_T and $D_{f,w}$ (or $D_{f,g}$), and there is no any empirical constant in this fractal relative permeability model.

4. Results and discussion

4.1. Phase fractal dimensions

The fractal theory requires that the values of fractal dimensions $D_{f,w}$ and $D_{f,g}$ be in the range of 1 and 2 in two dimensions based on the definition given by Eq. (2). To be valid, we first check/calculate the fractal dimensions $D_{f,w}$ and $D_{f,g}$. For this purpose, we take bi-dispersed porous media (Yu and Cheng, 2002) as samples for study because they have been proven to be fractal media.

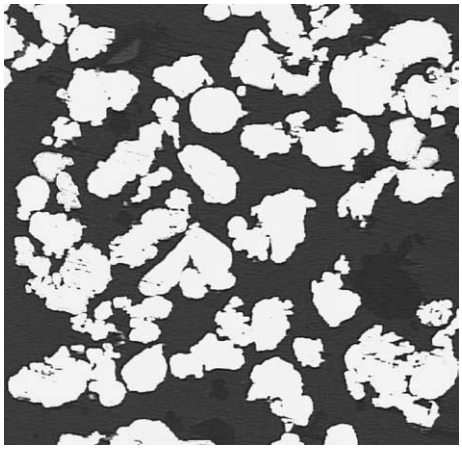

Fig. 2. An image photo (Yu and Cheng, 2002) of a bi-dispersed medium at porosity 0.54, where the black and the white regions are pores and clusters formed by agglomeration of copper particles. Since the micropores inside clusters are very small and the copper particles are soft, it is difficult to see the micropores inside clusters after the sample being polished.

The bi-dispersed porous structure, as shown in Fig. 2, is composed of clusters (at macrolevel), which are agglomerated by small particles (at microlevel). Since the clusters and particles within the clusters are randomly distributed, this leads to macropores and micropores of various sizes in a bi-dispersed porous medium, so this medium is much similar to packed beds. For saturated (or single-phase) bi-dispersed porous media, the pore area fractal dimension D_f can be described by Eq. (9). In Eq. (9), we roughly take $\lambda_{max}/\lambda_{min} = 24$, which is the same as the ratio (Yu and Cheng, 2002) of the average cluster size to the minimum particle size. Fig. 3 illustrates the results of pore area fractal dimension D_f versus porosity by Eq. (9) and by the box-counting method (Yu and

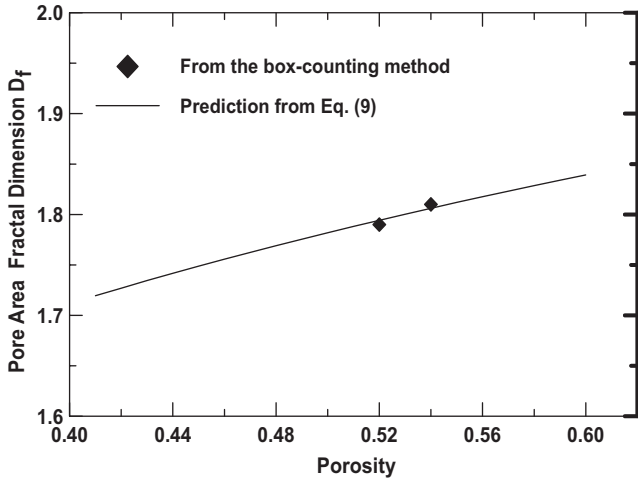

Fig. 3. A comparison between the theoretical predictions by Eq. (9) and the results from the box-counting method (Yu and Cheng, 2002).

Cheng, 2002). Fig. 3 shows the good agreement between the model prediction from Eq. (9) and those from the box-counting method for the saturated bi-dispersed porous media.

The fractal dimensions, $D_{f,w}$ and $D_{f,g}$, can be determined by Eq. (10). Fig. 4 gives the fractal dimensions, $D_{f,w}$ and $D_{f,g}$, versus the saturation S_w at different porosities and by roughly taking $\lambda_{max}/\lambda_{min} = 24$ again. It is seen from Fig. 4 that the fractal dimension $D_{f,w}$ increases monotonously with saturation. As saturation tends to 1 the fractal dimension $D_{f,w}$ reaches its maximum value of 1.80 at porosity 0.54, approximately the same value as the value 1.81 from the box-counting method for bi-dispersed medium at porosity 0.54 (Yu and Cheng, 2002). The similar phenomenon can be observed for non-wetting phase. The non-wetting phase fractal dimension $D_{f,g}$ reaches its maximum possible value 1.80 as saturation is zero at porosity 0.54. This means that as saturation tends to zero, the medium is fully filled with a non-wetting fluid (or single-phase fluid), so it is expected that fractal dimension is exactly the same as that for saturated porous medium. Fig. 4 also shows that the phase fractal dimension depends on porosity. The higher the porosity, the higher the fractal dimension. This can be interpreted that the higher porosity implies larger pore area, the larger pore area leads to the larger phase area/volume and the higher fractal dimension. In the limiting case, as porosity tends to 1, a unit cell of the medium becomes a smooth plane, whose fractal dimension is 2. Therefore, the present results are reasonable. From Fig. 4 an important phenomenon can be also found. That is when saturation $S_w < 0.1$, the fractal dimension $D_{f,w} < 1$. This reveals that when saturation $S_w < 0.1$, the wetting phase distribution in porous media is non-fractal (in two dimensions) according to fractal theory. Similarly, when saturation $S_w > 0.9$, $D_{f,g} < 1$. This indicates that the non-wetting phase distribution is also non-fractal (in two dimensions) when $S_w > 0.9$. This suggests that only when $S_w > 0.1$ and $S_w < 0.9$, the wetting and non-wetting phases are fractal objects, respectively. On the other hand, according to the literature by Kaviany (1995), at very low saturations the wetting phase becomes disconnected (or immobile), and at very high saturations the non-wetting phase becomes disconnected. This implies that at low saturations for wetting phase and at high saturations for non-wetting phase, the pore fluid is embedded in one dimension and the fractal dimension is less than one, and the fluid is

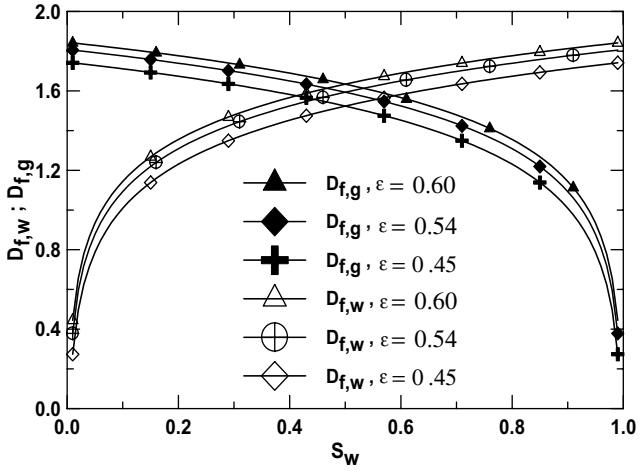

Fig. 4. The phase fractal dimensions versus saturation.

disconnected. Usually, the experimentally relative permeability data (De Wiest, 1969; Bear, 1972; Kaviany, 1995) were reported also in the range of about $S_w > 0.1$ for wetting phase. It is seen that the present fractal permeability results are consistent with the experimental observations, and the present analysis is thus restricted in the ranges of $S_w > 0.1$ for wetting phase and $S_w < 0.9$ for non-wetting phase for requirements from both fractal theory and experimental observations.

4.2. Fractal relative permeabilities

According to the above analysis, the present fractal relative permeabilities are given in the ranges of $S_w > 0.1$ for wetting phase and $S_w < 0.9$ for non-wetting phase.

The algorithm for determination of the relative permeabilities for unsaturated porous media is summarized as follows:

1. Select a porosity, ε.
2. Find D_f from Eq. (9).
3. Select a saturation, S_w, find $D_{f,w}$ and $D_{f,g}$ from Eqs. (10a) and (10b), respectively.
4. Find the relative permeabilities from Eqs. (37) and (38) ($D_T = 1.10$ is used in this work).

The above procedures 3 and 4 are repeated to find the relative permeabilities for a given porosity.

We have found that the above computation of relative permeabilities takes less than one second in a microcomputer, and no grid generation and no boundary conditions are needed. While applying any numerical method such as finite difference method, finite element method, lattice Boltzmann method and Monte Carlo simulation, grid generation and/or boundary conditions are needed, and thus much more computer time is often required. Therefore, the advantage of the present fractal analysis of permeabilities for porous media over numerical methods is evident.

Fig. 5 presents the relative permeabilities, k_{rw} and k_{rg}, versus saturation calculated from Eqs. (37) and (38), respectively. Fig. 5 shows that although the phase fractal dimensions depend on

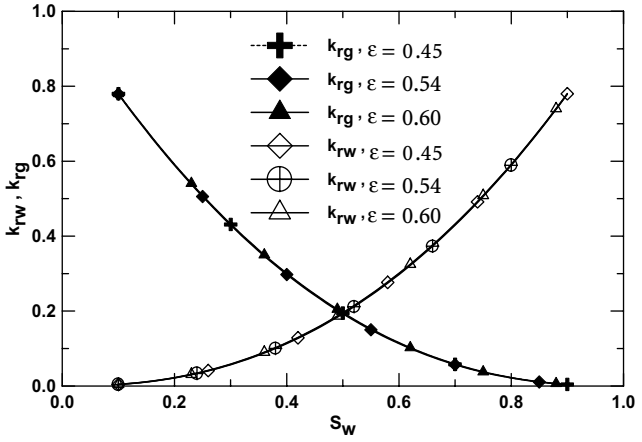

Fig. 5. The relative permeabilities predicted by the present fractal model.

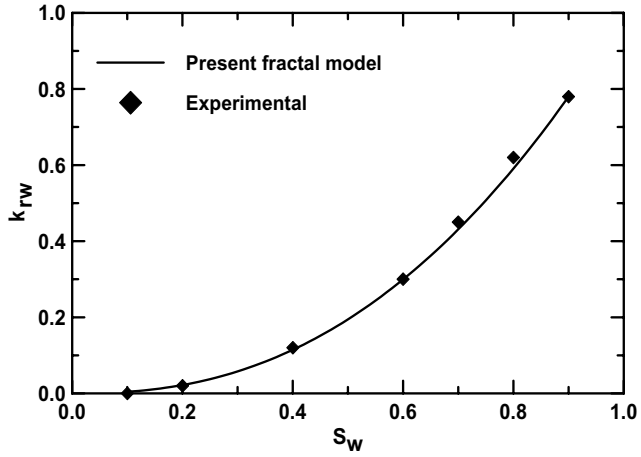

Fig. 6. A comparison of the relative permeabilities between the present fractal model predictions Eq. (37) and the existing experimental data (Levec and Saez, 1986; Kaviany, 1995).

porosity (see Fig. 4), the relative permeabilities predicted from Eqs. (37) and (38) are independent of porosity and are a function of saturation only. So, in this work, we approximately consider the bi-dispersed porous media as mono-dispersed porous media (similar to packed beds) in calculating the relative permeabilities. The present fractal relative permeability results are consistent with many empirical formulas, which are often expressed as a function of saturation with one or more empirical constants from experiments (Kaviany, 1995). However, there is no any empirical constant in the present fractal permeability models Eqs. (37) and (38), and this is an another advantage of the present fractal analysis over those empirical correlations from experiments and numerical simulations. From Fig. 5 it can be also found that $k_{rw} + k_{rg} < 1$, this is in consistence with general observations and the shapes of the relative permeability curves are also in consistence with the literature reports (De Wiest, 1969; Bear, 1972; Kaviany, 1995).

It should be noted that although the particles in a packed bed may be uniform in size, the capillaries in a packed bed are usually *non*-uniform and they may follow the fractal distribution. Fig. 6 compares the predictions from the present fractal permeability model for mono-dispersed porous media (similar to packed beds) and the experimental data (Kaviany, 1995; Levec and Saez, 1986) for packed beds, and excellent agreement between the predictions from the present fractal permeability model and the experimental data is obtained. This verifies the validity of the present fractal analysis of permeabilities for unsaturated porous media.

5. Concluding remarks

In this paper, a theoretical analysis of permeabilities for unsaturated porous media is presented based on the fractal characters of pore size/phase distributions in unsaturated porous media. The general phase fractal permeability models, given by Eqs. (16) and (17), are in terms of the fractal dimension D_T for tortuosity, pore area fractal dimension D_f, fractal dimensions $D_{f,w}$ for wetting

phase and $D_{f,g}$ for non-wetting phase, saturation S_w, and the structural parameters A, λ_{max}, L_0. The fractal relative permeability models given by Eqs. (37) and (38) are expressed as a function of the fractal dimensions D_T, D_f, $D_{f,w}$ and $D_{f,g}$, and saturation S_w. There is no any empirical constant in the present relative permeability models. The results from the present relative permeability models are found to be independent of porosity. The fractal permeability model Eq. (20) can be considered as a special case of the unsaturated porous medium by setting $S_w = 1$ in Eqs. (10a) and (36a) or by setting $S_w = 0$ in Eqs. (10b) and (36c). The predictions of the relative permeabilities of porous media based on the proposed fractal model are found to be in excellent agreement with existing experimental data. This verifies the validity of the present fractal analysis of permeability for porous media.

Acknowledgement

This work was supported by the National Natural Science Foundation of China through Grant Numbers 10272052.

References

Adler, P.M., 1985. Transport processes in fractals—I. Conductivity and permeability of a Leibniz packing in the lubrication limit. Int. J. Multiphase Flow 11, 91–108.

Adler, P.M., 1996. Transports in fractal porous media. J. Hydrol. 187, 195–213.

Adler, P.M., Berkowitz, B., 2000. Effective medium analysis of random lattices. Transport Porous Media 40, 145–151.

Adler, P.M., Thovert, J.-F., 1998. Real porous media: local geometry and macroscopic properties. Appl. Mech. Rev. 51, 537–585.

Bear, J., 1972. Dynamics of Fluids in Porous Media. American Elsevier Publishing Company, Inc.

Benzi, R., Succi, S., Vergassola, M., 1992. The lattice Boltzmann equation: theory and applications. Phys. Rep. 222, 145–197.

Bowles, J., 1984. Physical and Geotechnical Properties of Soil, second ed. McGraw-Hill Book Company, New York.

Chen, S., Doolen, G.D., 1998. Lattice Boltzmann method for fluid flows. Annu. Rev. Fluid Mech. 30, 329–364.

Chen, Z.Q., Cheng, P., Zhao, T.S., 2000. An experimental study of two phase flow and boiling heat transfer in bidispersed porous channels. Int. Commun. Heat Mass Transfer 27, 293–302.

De Wiest, R.J.M., 1969. Flow through Porous Media. Academic Press, New York and London.

Denn, M.M., 1980. Process Fluid Mechanics. Prentice Hall, NJ. pp. 35.

Feder, J., 1988. Fractals. Plenum Press, New York. pp. 7–30,184–192.

Jumikis, A.R., 1984. Soil Mechanics. Robert E. Krieger Publishing Company, Inc., Malabar, Florida.

Katz, A.J., Thompson, A.H., 1985. Fractal sandstone pores: Implications for conductivity and pore formation. Phys. Rev. Lett. 54, 1325–1328.

Kaviany, M., 1995. Principles of Heat Transfer in Porous Media, second ed. Springer-Verlag, New York.

Krohn, C.E., Thompson, A.H., 1986. Fractal sandstone pores: Automated measurements using scanning-electron-microscope images. Phys. Rev. B 33, 6366–6374.

Levec, J., Saez, A.E., 1986. The hydrodynamics of Tricking flow in packed beds. Part II: Experimental observations. AIChE J. 32, 369–380.

Majumdar, A.A., Bhushan, B., 1990. Role of fractal geometry in roughness characterization and contact mechanics of surfaces. J. Tribol. 112, 205–216.

Mandelbrot, B.B., 1982. The Fractal Geometry of Nature. Freeman, San Francisco. pp. 15, 23–57,117–119.

Martys, N.S., Chen, H., 1996. Simulation of multicomponent fluids in complex three-dimensional geometries by the lattice Boltzmann method. Phys. Rev. E 53, 743–750.

Muskat, M., Meres, A.W., 1936. The flow of heterogeneous fluid through porous media. Physics 7, 346–363.
Ngo, N.D., Tamma, K.K., 2001. Microscale permeability predictions of porous fibrous media. Int. J. Heat Mass Transfer 44, 3135–3145.
Onoda, G.Y., Toner, J., 1986. Fractals dimensions of model particle packings having multiple generations of agglomerations. J. Am. Ceram. Soc. 69, C278–C279.
Pandey, R.B., Becklehimer, J.L., Gettrust, J.F., 2001. Density profile and flow of driven gas in an open porous medium with a computer simulation. Physica A 289, 321–335.
Panfilov, M., 2000. Macroscale Models of Flow through Highly Heterogeneous Porous Media. Kluwer Academic Pub, London.
Perfect, E., Kay, B.D., 1991. Fractal theory applied to soil aggregation. Soil Sci. Soc. Am. J. 55, 1552–1558.
Pitchumani, R., Ramakrishnan, B., 1999. A fractal geometry model for evaluating permeabilities of porous preforms used in liquid composite molding. Int. J. Heat Mass Transfer 42, 2219–2232.
Sasaki, A., Aiba, S., Fukuda, H., 1987. A study on the thermophysical properties of a soil. ASME, J. Heat Transfer 109, 232–237.
Shih, C.-H., Lee, L.J., 1998. Effect of fiber architecture on permeability in liquid composite molding. Polym. Compos. 19, 626–639.
Smidt, J.M., Monro, D.M., 1998. Fractal modeling applied to reservoir characterization and flow simulation. Fractals 6, 401–408.
Wang, T.J., Wu, C.H., Lee, L.J., 1994. In-plane permeability measurement and analysis in liquid composite molding. Polym. Compos. 15, 278–288.
Wheatcraft, S.W., Tyler, S.W., 1988. An explanation of scale-dependent dispersivity in heterogeneous aquifers using concepts of fractal geometry. Water Resour. Res. 24, 566–578.
Wu, C.-H., Wang, T.J., Lee, L.J., 1994. Trans-plane fluid permeability measurement and its application in liquid composite molding. Polym. Compos. 15, 289–298.
Young, I.M., Crawford, J.W., 1991. The fractal structure of soil aggregations: its measurement and interpretation. J. Soil Sci. 42, 187–192.
Yu, B.M., 2001. Comments on "A fractal geometry model for evaluating permeabilities of porous preforms used in liquid composite molding". Int. J. Heat Mass Transfer 44, 2787–2789.
Yu, B.M., Cheng, P., 2002. A fractal permeability model for bi-dispersed porous media. Int. J. Heat Mass Transfer 45, 2983–2993.
Yu, B.M., Lee, L.J., 2000. A simplified in-plane permeability model for textile fabrics. Polym. Compos. 21, 660–685.
Yu, B.M., Li, J.H., 2001. Some fractal characters of porous media. Fractals 9, 365–372.
Yu, B.M., Lee, L.J., Cao, H.Q., 2001. Fractal characters of pore microstructures of textile fabrics. Fractals 9, 155–163.
Yu, B.M., Lee, L.J., Cao, H.Q., 2002. A fractal in-plane permeability model for fabrics. Polym. Compos. 23, 201–221.
Yu, B.M., Li, J.H., Zhang, D.M., 2003. A fractal trans-plane permeability model for textile fabrics. Int. Commun. Heat Mass Transfer 30, 127–138.
Yu, B.M., Li, J.H. Fractal dimensions for unsaturated porous media. Fractals, in press.